

Characteristics of 1–3-type ferroelectric ceramic/auxetic polymer composites

V Yu Topolov^{1,2} and C R Bowen²

¹ Department of Physics, Southern Federal University, 5 Zorge Street, 344090 Rostov-on-Don, Russia

² Materials Research Centre, Department of Mechanical Engineering, University of Bath, Bath BA2 7AY, UK

E-mail: topolov@phys.rsu.ru and c.r.bowen@bath.ac.uk

Received 18 August 2007, in final form 19 October 2007

Published 13 December 2007

Online at stacks.iop.org/MSMSE/16/015007

Abstract

This paper presents modelling and simulation results on 1–3 piezoactive composites comprising a range of ferroelectric ceramics, which are assumed to have variable properties and an auxetic polymer (i.e. a material with a negative Poisson ratio) that improves the hydrostatic piezoelectric response of the composite. Dependences of the effective piezoelectric coefficients and related parameters of the 1–3 composites on the degree of poling, mobility of the 90° domain walls within ceramic grains, on the volume fraction of the ceramic component and on the Poisson ratio of the polymer component have been calculated and analysed. The role of the piezoelectric anisotropy and domain-orientation processes in improving and optimising the effective parameters, piezoelectric activity and sensitivity of 1–3 ferroelectric ceramic/auxetic composites is discussed.

1. Introduction

Piezoactive composites with 1–3 connectivity can be considered as ferroelectric ceramic (FC) or single-crystal rods embedded in a polymer matrix [1–3]. The design, manufacture and performance of the 1–3 and related FC/polymer composites have been the subject of a considerable number of studies in recent decades (see, e.g. papers [1, 2, 4–6]). The 1–3 piezocomposites are of particular interest since they provide excellent effective electromechanical (i.e. elastic, piezoelectric and dielectric) properties for utilisation as active elements of transducers, medical ultrasonic imaging devices, hydrophones and other piezotechnical devices [3–5]. It has been shown that by combining the advantages of both ceramic and polymer components, optimising the microgeometry of the composite and taking into account an effectiveness of stress transfer from the polymer matrix to the rods, it is possible to produce high performance 1–3-type composites [2, 4, 5, 7] with properties superior

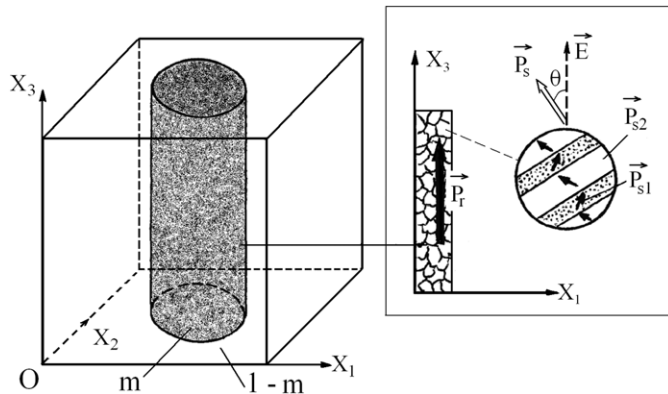


Figure 1. Schematic representation of the 1–3 composite. ($X_1X_2X_3$) is the rectangular co-ordinate system. m and $1 - m$ are volume fractions of the FC and polymer components, respectively. In the inset a FC rod with the remanent polarisation P_r is shown. P_{s1} and P_{s2} are the spontaneous polarisation vectors of the 90° domains in a FC grain and E is the poling field vector.

to monolithic piezoelectric materials. The possibilities of increasing the piezoelectric response of the 1–3-type composite are often concerned with creating a porous structure in the polymer matrix [7–10] or choosing the optimum FC component [10]. Of specific interest for this paper is the use of a matrix material based on auxetic polymers with negative Poisson's ratios [7–9, 11, 12]. It is known that an auxetic material expands laterally when stretched, in contrast to ordinary materials with a positive Poisson ratio. The first isotropic auxetic polymer was manufactured and studied by Lakes [13] two decades ago. Due to a foam structure with open cells, the Poisson ratio in this polymer was -0.7 [13] while most isotropic polymers have a Poisson ratio of approximately 0.3 [11]. In general, all isotropic materials obey the law of conservation of energy, show a positive definite matrix of elastic compliances and, as a consequence, can have the Poisson ratio in the range from -1 to 0.5 [11, 13].

Current literature data on the 1–3-type piezocomposites has not attempted to understand the influence of changes in the electromechanical properties of the FC on the piezoelectric response of composites having auxetic polymer matrices. In this paper we consider the changes caused mainly by poling either the FC or 90° domain-wall displacements within FC grains. The aim of this work is to demonstrate and understand how the piezoelectric performance and the potential benefits of a FC/auxetic polymer composite depend on the above-mentioned changes in the FC properties.

2. Determination of effective electromechanical properties in composites

2.1. Model concepts

Our analysis is carried out within the framework of a model based on a 1–3 composite that consists of a system of extended FC rods running parallel to the poling axis OX_3 (figure 1) which are surrounded by a continuous auxetic polymer matrix. The FC rods are in the form of circular cylinders which are regularly distributed over a composite sample so that there is a square arrangement of the rods in the (X_1OX_2) plane. Changes in the electromechanical properties of the FC rods can occur for a number of reasons. Firstly, during poling of the 1–3 composite under an electric field $E \parallel OX_3$ a monotonic increase of the remanent polarisation P_r

in the FC is closely connected with a rotation of the spontaneous polarisation vector \mathbf{P}_s in the polydomain ceramic grain (figure 1, inset). Secondly, non-180° domain-wall displacements can occur within ceramic grains, even under the application of a relatively weak electric field or mechanical stress. Such domain displacements can provide considerable contribution to the electromechanical constants of the FC, as has been shown for the tetragonal phase BaTiO₃ (BT) FC [14]. It is assumed that 180° domain reversals have been fully completed during poling and regular laminar 90° domain structures (figure 1, inset) are present in all the grains of the tetragonal composition. The spontaneous polarisation \mathbf{P}_s of each grain is expressed as follows: $\mathbf{P}_s = m_{s1}\mathbf{P}_{s1} + (1 - m_{s1})\mathbf{P}_{s2}$ where m_{s1} is the volume fraction of the domain type with the spontaneous polarisation \mathbf{P}_{s1} . In this paper we consider the rotation of the \mathbf{P}_s vector at $m_{s1} = 1/2$ and the 90° domain-wall displacements starting in polydomain grains also with $m_{s1} = 1/2$.

The angle $\Theta = (\mathbf{P}_s, \hat{\mathbf{E}})$ for an individual grain (figure 1, inset) can vary from 0 to Θ_l , and the remanent polarisation P_r in the FC component is characterised [15, 16] by a maximum angle Θ_l . Since the poling process results in increasing P_r and decreasing Θ_l , it is convenient to introduce an angle $\Theta' = 180^\circ - \Theta_l$ [15] that would increase monotonically on increasing P_r . It should be added that values $\Theta_l < 45^\circ$ cannot be attained in the fully poled FC with the above-described ceramic grains split into the 90° domains [15].

2.2. Averaging procedures and electromechanical properties in components

The electromechanical constants of the FC and polymer components are denoted with superscripts (1) and (2), respectively. The effective electromechanical properties of the 1–3 composites are determined in the long-wave approximation as a function of the volume fraction m of the FC by the effective field method. This method is regarded as the Mori–Tanaka method [17] generalised for piezoactive media [18] or as one of the variants of the self-consistent scheme [19]. In the averaging procedure the electromechanical interaction between the piezoactive FC rods in the matrix and related coupled effects are taken into account. There are a variety of methods [1, 2, 11, 19–21] to calculate the full set of the effective electromechanical constants and to take into account the aforementioned electromechanical interaction. These schemes have been applied to the 1–3 FC/polymer composites with one (FC rods) or two piezoelectric components. Calculations are carried out using various sets of the electromechanical constants of the components, for example, elastic moduli $c_{ab}^{(n),E}$ measured at $E = \text{const}$, piezoelectric coefficients $e_{ij}^{(n)}$ and dielectric constants $\varepsilon_{pp}^{(n),\xi}$ measured at mechanical strain $\xi = \text{const}$ or elastic compliances $s_{ab}^{(n),E}$, piezoelectric coefficients $d_{ij}^{(n)}$ and dielectric constants $\varepsilon_{pp}^{(n),\sigma}$ measured at mechanical stress $\sigma = \text{const}$, where $n = 1$ or 2.

The electromechanical properties in the FC component with a variable remanent polarisation are determined in two stages. Following an algorithm from the work [15], the electromechanical constants of the polydomain grain (figure 1, inset) are initially calculated as a function of m_{s1} by means of a piecewise method of uniform fields [22]. In this method the boundary conditions for electric and mechanical fields are taken into account for the adjacent domains that form the regular laminar 90° domain structure. In the second stage the electromechanical constants $s_{ab}^{(1),E}$, $d_{ij}^{(1)}$ and $\varepsilon_{pp}^{(1),\sigma}$ of the FC are determined as a result of averaging the electromechanical constants of the polydomain grains over all allowable orientations of \mathbf{P}_s , i.e. $0 \leq (\mathbf{P}_s, \hat{\mathbf{E}}) \leq \Theta_l$. This averaging is implemented within the framework of the self-consistent scheme (effective medium method) [22, 23] that takes into account the electromechanical interaction between the piezoactive grains.

Table 1. Elastic moduli $c_{ab}^{(1),E}$ (in 10^{10} Pa), piezoelectric coefficients $e_{ij}^{(1)}$ (in $C\text{ m}^{-2}$) and dielectric constants $(\epsilon_{pp}^{(1),\xi}/\epsilon_0)$ of $(\text{Pb}_{0.76}\text{Ca}_{0.24})\text{TiO}_3$ ferroelectric ceramics with a variable remanent polarisation.

Θ' ($^\circ$)	Θ_l ($^\circ$)	$c_{11}^{(1),E}$	$c_{12}^{(1),E}$	$c_{13}^{(1),E}$	$c_{33}^{(1),E}$	$c_{44}^{(1),E}$	$e_{31}^{(1)}$	$e_{33}^{(1)}$	$e_{15}^{(1)}$	$\epsilon_{11}^{(1),\xi}/\epsilon_0$	$\epsilon_{33}^{(1),\xi}/\epsilon_0$
0	180	18.2	4.26	4.19	17.8	7.02	0	0	0	150	150
10	170	18.2	4.26	4.21	17.8	7.03	0.0150	0.0701	0.0272	150	150
20	160	18.3	4.24	4.25	17.9	7.03	0.0600	0.278	0.108	150	150
30	150	18.4	4.22	4.32	18.0	7.04	0.136	0.619	0.241	150	149
40	140	18.5	4.21	4.38	18.1	7.03	0.235	1.08	0.422	150	149
50	130	18.6	4.20	4.42	18.2	7.03	0.372	1.65	0.644	150	148
60	120	18.6	4.21	4.45	18.2	7.01	0.527	2.30	0.906	150	147
70	110	18.6	4.21	4.38	18.1	6.99	0.689	3.01	1.19	149	146
80	100	18.5	4.22	4.26	17.8	6.98	0.850	3.75	1.50	149	145
90	90	18.2	4.24	4.07	17.3	6.96	1.00	4.48	1.81	148	144
100	80	17.9	4.27	3.84	16.6	6.95	1.13	5.17	2.13	146	144
110	70	17.5	4.34	3.57	15.8	6.92	1.23	5.81	2.42	145	143
120	60	17.2	4.47	3.29	15.1	6.87	1.30	6.38	2.69	143	142
125	55	17.1	4.55	3.15	14.7	6.84	1.32	6.65	2.81	142	142
130	50	17.0	4.64	3.01	14.3	6.79	1.34	6.88	2.92	141	142
135	45	16.9	4.75	2.90	14.1	6.75	1.35	7.11	3.02	141	142

Note 1. The electromechanical constants of the single-domain crystal have been evaluated by the method from the work of [23] on the basis of experimental data on $(\text{Pb}_{1-x}\text{Ca}_x)\text{TiO}_3$ solid solutions at room temperature.

Note 2. For the poled FC with ∞mm symmetry, $c_{66}^{(1)} = (c_{11}^{(1),E} - c_{12}^{(1),E})/2$ [26].

2.3. Materials (FC and polymer)

Three different FC components have been chosen with a variety of degrees of polarisation to provide a range of possible responses. The corresponding calculations have been made for two PbTiO_3 -type FCs, namely, $(\text{Pb}_{0.76}\text{Ca}_{0.24})\text{TiO}_3$ (PCT) and $\text{Pb}(\text{Zr}_{0.1}\text{Ti}_{0.9})\text{O}_3$ (PZT), on assumption [23] that the 90° domain walls are motionless. It is known from the experimental studies [24] that the 90° domain structure in the PbTiO_3 FC grains shows limited sensitivity to the action of strong mechanical or electric fields. The PCT FC is of interest for transducer applications due to the large anisotropy of the piezoelectric coefficients $d_{3j}^{(1)}$ (i.e. $d_{33}^{(1)}/|d_{31}^{(1)}| \gg 1$) [23, 25] and the positive signs of the piezoelectric coefficients $e_{3j}^{(1)}$ (table 1). The PZT FC shows a less-pronounced anisotropy of $d_{3j}^{(1)}$ and a non-monotonic behaviour of $e_{3j}^{(1)}(\Theta')$; however, the piezoelectric coefficient $e_{31}^{(1)}$ passes the zero value twice (table 2) on increasing the angle Θ' and provides a ratio of $|e_{33}^{(1)}/|e_{31}^{(1)}| > 10$ in a wide Θ' range. It should be noted that Smith [27] first presented results on modelling the effective electromechanical properties and the hydrostatic piezoelectric response of the 1–3 FC/polymer composites based on either $(\text{Pb}, \text{Ca})\text{TiO}_3$ FC (with $d_{33}^{(1)}/|d_{31}^{(1)}| \approx 29$) or PZT-5 FC (with $d_{33}^{(1)}/|d_{31}^{(1)}| \approx 2.2$). Three sets of experimental electromechanical constants of the components were used to study the volume fraction dependences of the effective parameters of the 1–3 composites with an ordinary (non-auxetic) polymer matrix [27].

In this study we also used the electromechanical constants calculated for the BT FC [28] by taking into account elastic 90° domain-wall displacements in ceramic grains. This calculation has been made within the framework of a model [28] of a single crystal split into 90° domains separated by planar movable domain walls. Spontaneous polarisation vectors of these domains are written in the rectangular co-ordinate system $(X_1^0 X_2^0 X_3^0)$ as $\mathbf{P}_{s1}(-P, 0, P)$ and $\mathbf{P}_{s2}(P, 0, P)$. The 90° domain-wall displacements appear along the OX_3^0 axis under an external electric or mechanical field and cause an orientation contribution to the electromechanical constants of

Table 2. Elastic moduli $c_{ab}^{(1),E}$ (in 10^{10} Pa), piezoelectric coefficients $e_{ij}^{(1)}$ (in $C\text{ m}^{-2}$) and dielectric constants ($\varepsilon_{pp}^{(1),\xi}/\varepsilon_0$) of $\text{Pb}(\text{Zr}_{0.1}\text{Ti}_{0.9})\text{O}_3$ ferroelectric ceramics with a variable remanent polarisation.

$\Theta' (\circ)$	$\Theta_l (\circ)$	$c_{11}^{(1),E}$	$c_{12}^{(1),E}$	$c_{13}^{(1),E}$	$c_{33}^{(1),E}$	$c_{44}^{(1),E}$	$e_{31}^{(1)}$	$e_{33}^{(1)}$	$e_{15}^{(1)}$	$\varepsilon_{11}^{(1),\xi}/\varepsilon_0$	$\varepsilon_{33}^{(1),\xi}/\varepsilon_0$
0	180	20.1	7.15	7.15	20.1	6.46	0	0	0	144	144
10	170	20.1	7.15	7.17	20.1	6.46	-0.00173	0.0701	0.0314	144	144
20	160	20.2	7.15	7.23	20.2	6.46	-0.00580	0.277	0.0673	144	143
30	150	20.3	7.16	7.31	20.3	6.46	-0.00943	0.610	0.281	144	143
40	140	20.4	7.18	7.41	20.4	6.45	-0.00850	1.05	0.498	144	142
50	130	20.6	7.20	7.51	20.5	6.45	-0.00220	1.59	0.769	144	141
60	120	20.6	7.22	7.55	20.5	6.44	0.0110	2.20	1.09	143	140
70	110	20.6	7.22	7.51	20.4	6.42	0.0254	2.86	1.44	143	139
80	100	20.4	7.20	7.38	20.1	6.40	0.0352	3.54	1.82	141	138
90	90	20.1	7.15	7.15	19.6	6.37	0.0341	4.25	2.20	139	137
100	80	19.6	7.09	6.84	19.0	6.34	0.0107	4.95	2.57	137	137
110	70	19.2	7.13	6.73	19.0	6.30	0.0383	5.84	2.90	135	136
120	60	18.6	7.03	6.14	17.5	6.25	-0.111	6.27	3.20	132	136
125	55	18.4	7.09	6.00	17.2	6.23	-0.151	6.58	3.32	131	135
130	50	18.2	7.06	5.82	16.8	6.21	-0.205	6.85	3.44	130	135
135	45	18.0	7.10	5.69	16.4	6.18	-0.253	7.12	3.53	129	135

Note 1. The electromechanical constants of the single-domain crystal have been evaluated by the method from work [23] on the basis of experimental data on $\text{Pb}(\text{Zr}_{1-x}\text{Ti}_x)\text{O}_3$ solid solutions at room temperature.

Note 2. For the poled FC with ∞mm symmetry, $c_{66}^{(1)} = (c_{11}^{(1),E} - c_{12}^{(1),E})/2$ [26].

the single crystal. According to Aleshin [28], there are three orientation contributions as follows: $\Delta\varepsilon_{11}^\sigma = 2P_s^2/(Hc)$ into the dielectric permittivity, $\Delta d_{15} = 4P_s(\xi_{33}^s - \xi_{11}^s)/(\sqrt{2}Hc)$ into the piezoelectric coefficient and $\Delta s_{55}^E = 4(\xi_{33}^s - \xi_{11}^s)/(Hc)$ into the elastic compliance where $P_s = |\mathbf{P}_{s1}| = |\mathbf{P}_{s2}|$; ξ_{jj}^s is the spontaneous strain of the domain in the OX_j^0 direction, H is the average width of the 90° domain and c is a parameter involved in an equilibrium equation $cx = f$. In this equation x is a domain-wall displacement and f is a thermodynamic pressure that acts on the domain wall under weak external fields. To calculate the full set of the electromechanical constants $s_{ab}^{(1),E}$, $d_{ij}^{(1)}$ and $\varepsilon_{pp}^{(1),\sigma}$ of the FC, it is reasonable to introduce a parameter $\gamma = (Hc)^{-1} \times 10^6$ Pa [28] that describes a mobility of the 90° domain walls within the proposed model. However, before this calculation, the electromechanical constants $s_{ab}^{\text{DS},E}$, d_{ij}^{DS} and $\varepsilon_{pp}^{\text{DS},\sigma}$ are determined [29] for the single crystal with the regular 90° domain structure on the assumption that all the 90° domain walls are immovable. The electromechanical constants of the polydomain single crystal with the movable 90° domain walls are represented as $s_{ab}^{\text{DS},E} + \Delta s_{ab}^E$, $d_{ij}^{\text{DS}} + \Delta d_{ij}$ and $\varepsilon_{pp}^{\text{DS},\sigma} + \Delta\varepsilon_{pp}^\sigma$ and hereafter involved in the averaging procedure. This procedure allowing for an anisotropy of the FC medium and an electromechanical interaction between the FC grains [28] is based on the self-consistent scheme (the effective medium method) [30]. It is assumed that all the grains have a spherical shape and similar 90° domain structures with individual orientations of the main crystallographic axes with respect to the $(X_1^0 X_2^0 X_3^0)$ system. The calculated dependences $|s_{ab}^{(1),E}(\gamma)|$, $|d_{ij}^{(1)}(\gamma)|$ and $\varepsilon_{pp}^{(1),\sigma}(\gamma)$, which are related to the BT FC with tetragonal symmetry of the separate domain and used in our further predictions, monotonically increase [28] on increasing the γ value and the 90° domain-wall mobility in the FC grains.

The auxetic polymer matrix of the 1–3 composites studied here is assumed to be made of polymethacrylimide (PMI) which is a closed-cell foam material. According to room-temperature data [31], this material is characterised by Young's modulus $E^{(2)} = 259.93$ MPa, shear modulus $G^{(2)} = 149.96$ MPa and Poisson's ratio $\nu^{(2)} = -0.12$ and does not possess

piezoelectric properties. Due to the lack of data on the dielectric properties of auxetic PMI in the paper [31] and other works, the value of the dielectric constant used is $\varepsilon_{pp}^{(2)}/\varepsilon_0 = 3.5$ since it is a typical value of similar dense polymers (polyurethane, etc [8, 10]).

3. Results and discussion

The effective electromechanical constants of the 1–3 composites studied in this work have been calculated on the basis of the formulae proposed by Chan and Unsworth [1], Taunaumang *et al* [2], Grekov *et al* [20] (the effective field method, expressions in the explicit form) and Huang and Kuo [21] (the effective field method, matrix approach). The difference between the related constants calculated using the above-mentioned formulae for the FC fraction $m = \text{const}$ does not exceed 1% in the volume fraction range of $0 < m \leq 0.6$. In this study we focus our attention on the piezoelectric response that is characterised by the piezoelectric coefficients $d_{33}^*, g_{33}^* = d_{33}^*/\varepsilon_{33}^{*\sigma}$ and $(Q_{33}^*)^2 = d_{33}^*g_{33}^*$ as well as by hydrostatic (hydrophone) parameters $d_h^*, g_h^* = d_h^*/\varepsilon_{33}^{*\sigma}$ and $(Q_h^*)^2 = d_h^*g_h^*$. The piezoelectric coefficients d_{33}^* and d_h^* are used to describe the piezoelectric activity of the composite whereas the piezoelectric coefficients g_{33}^* and g_h^* are introduced to describe piezoelectric sensitivity. The squared figures of merit $(Q_{33}^*)^2$ and $(Q_h^*)^2$ are related to power densities and signal-to-noise ratios in piezoelectric transducers, hydrophones and other piezotechnical devices.

3.1. Results for PCT- and PZT-based composites

Examples of the dependence of the aforementioned effective parameters on the orientation angle Θ' , mobility factor γ and volume fraction m are shown in figures 2, 3 and 4, respectively. Small differences between the d_{33}^* curves related to different m values (see, e.g. curves 1 and 3 in figures 2(a) and (d)) are mainly the result of the significant differences between the elastic moduli $c_{ab}^{(1),E}$ and $c_{ab}^{(2)}$ of the stiff FC and compliant polymer components. As is known, the piezoelectric coefficient d_{33}^* of the 1–3 FC/polymer composite [1, 2, 20] increases rapidly with increasing m when $m \ll 1$ and then, on further increasing m , increases very slowly ($d_{33}^* \rightarrow d_{33}^{(1)}$).

Of interest is a similar behaviour of the d_{33}^* and d_h^* curves related to $m = \text{const}$ (compare curves 1 and 2 or 3 and 4 in figures 2(a) and (d)). It has been shown [1, 2, 20] that the piezoelectric coefficients d_{33}^* and d_h^* of the 1–3-type composite at small m values can be written in the following form: $d_{33}^*|_{m \ll 1} \approx md_{33}^{(1)}s_{11}^{(2)}(ms_{11}^{(2)} + s_{33}^{(1),E})^{-1}$ and

$$d_h^*|_{m \ll 1} \approx d_{33}^*|_{m \ll 1} + 2md_{33}^{(1)}[(d_{31}^{(1)}/d_{33}^{(1)})(ms_{11}^{(2)} + s_{33}^{(1),E}) + s_{12}^{(2)}](ms_{11}^{(2)} + s_{33}^{(1),E})^{-1}. \quad (1)$$

As follows from equation (1), the difference $(d_h^* - d_{33}^*)|_{m \ll 1}$ is highly dependent on $d_{31}^{(1)}/d_{33}^{(1)}$ (which has a negative value for the FCs considered in this study) and $s_{12}^{(2)}$, which has a positive value for auxetic polymers. The highly anisotropic PTC FC provides a small contribution into d_h^* from equation (1) due to small $|d_{31}^{(1)}/d_{33}^{(1)}|$ values over the wide Θ' range. In contrast to the PTC, the PZT FC is characterised by relatively large $|d_{31}^{(1)}/d_{33}^{(1)}|$ values which influence the balance of items from equation (1) and therefore the arrangements of curves 1–4 in figure 2(d). It can be seen from equation (1) that the item $s_{12}^{(2)} > 0$ for the auxetic polymer enables the composite to attain an inequality $d_h^* > d_{33}^*$ for the PTC/auxetic PMI composite (figure 2(a)). Since $d_h^* = d_{33}^* + 2d_{31}^*$, this implies that the auxetic matrix enables a positive d_{31}^* to be attained in the composite, which is not possible for monolithic FCs. The same inequality does not hold for the 1–3 PZT/polymer composites [1, 2, 10, 20] at $s_{12}^{(2)} < 0$ in their matrices.

In contrast to the small differences between the d_{33}^* curves (figures 2(a) and (d)), the piezoelectric coefficient g_{33}^* is varied in a wide range (see curves 1, 3, 5 and 7 in

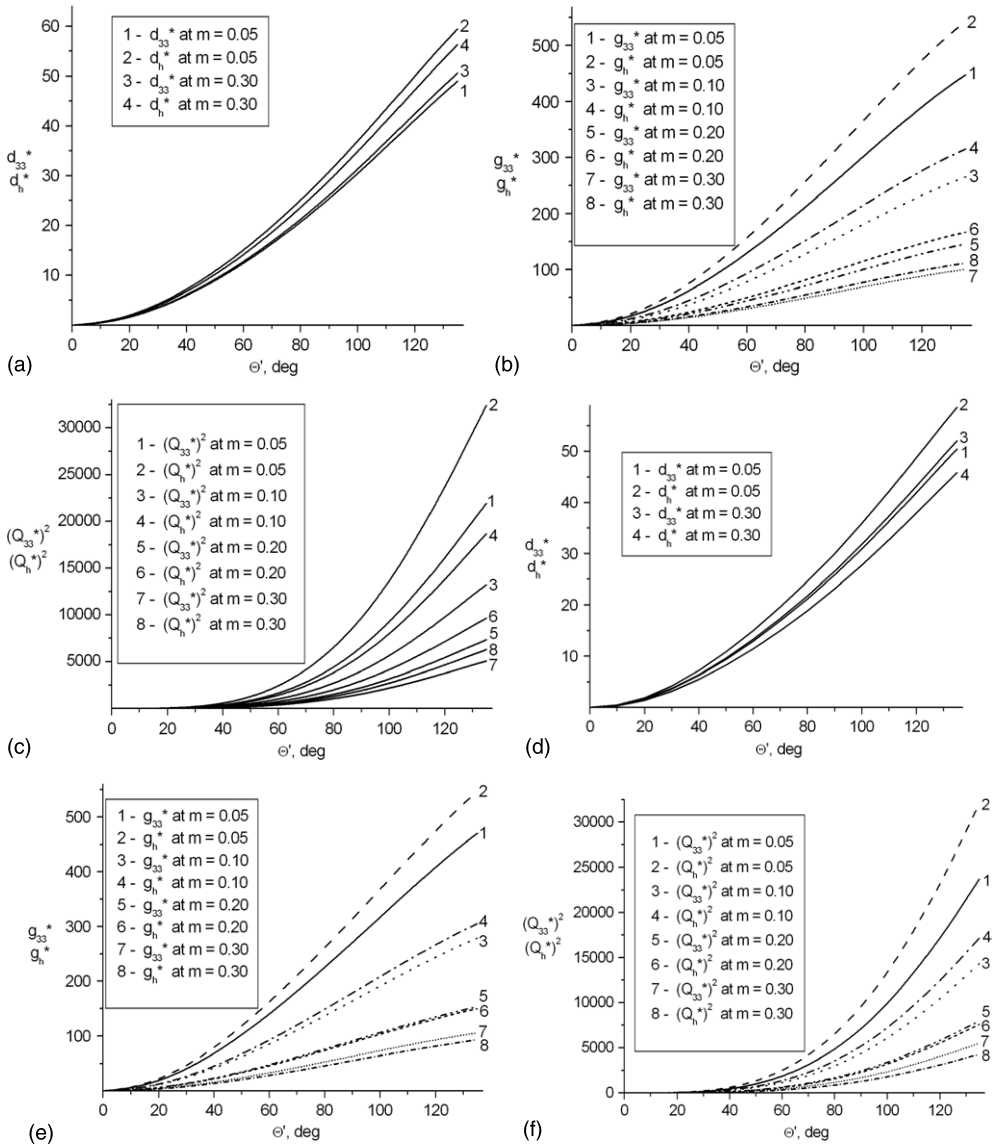


Figure 2. Effective parameters $\Phi^*(\theta')$ calculated for the 1–3-type PCT FC/auxetic PMI (a)–(c) and PZT FC/auxetic PMI (d)–(f) composites at $m = \text{const}$: piezoelectric coefficients d_{33}^* and d_h^* ((a) and (d) in pCN⁻¹), piezoelectric coefficients g_{33}^* and g_h^* ((b) and (e) in mV mN⁻¹) and squared figures of merit $(Q_{33}^*)^2$ and $(Q_h^*)^2$ ((c) and (f) in 10⁻¹⁵ Pa⁻¹).

figures 2(b) and (e)). This behaviour is associated with the influence of the dielectric constant $\varepsilon_{33}^{*\sigma}$ that monotonically increases on increasing m . The mutual arrangement and similar behaviour of the g_{33}^* and g_h^* curves is again accounted for by a competition between the items $s_{12}^{(2)} > 0$ and $(d_{31}^{(1)}/d_{33}^{(1)})(ms_{11}^{(2)} + s_{33}^{(1),E}) < 0$ from equation (1). In the cases of the PTC- and PZT-based composites the arrangement of the $(Q_{33}^*)^2$ and $(Q_h^*)^2$ curves is similar to that shown for the g_{33}^* and g_h^* curves, respectively (compare, e.g. figures 2(b) and (c) or figures 2(e) and (f)).

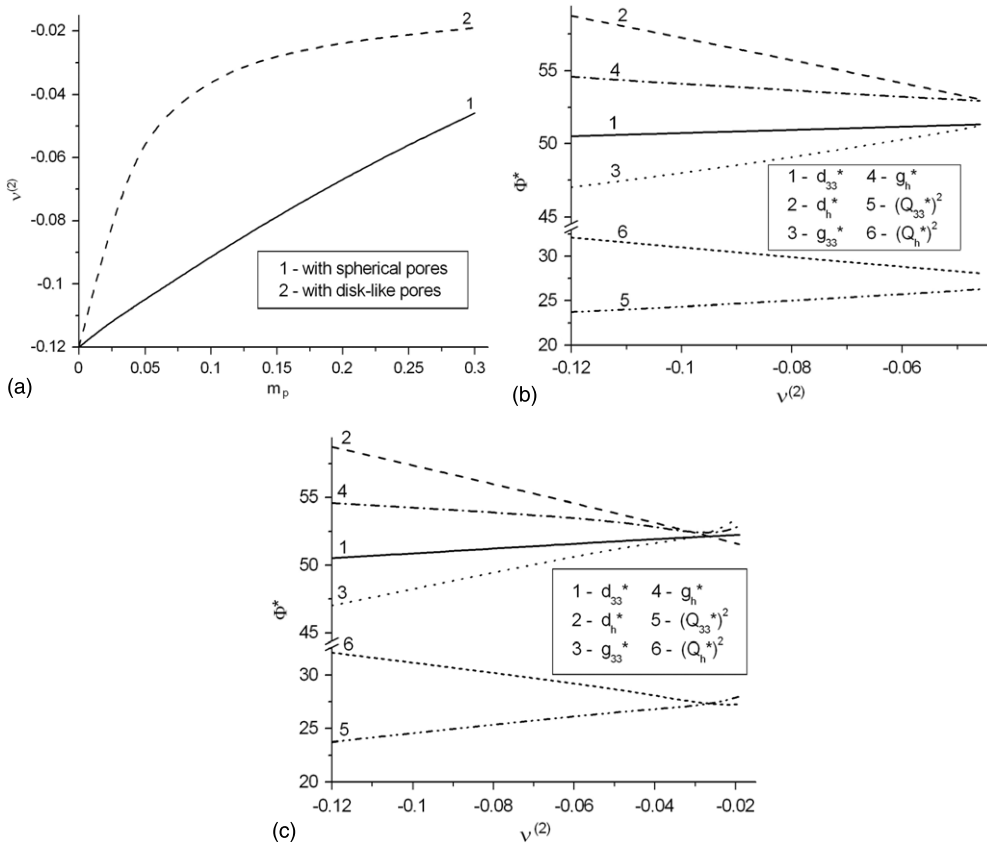


Figure 3. Poisson's ratio $\nu^{(2)}(m_p)$ of the porous and auxetic PMI matrix (a) and effective parameters $\Phi^*(\nu^{(2)})$ calculated for the 1–3-type PZT FC/porous and auxetic PMI composite ((b) and (c)) at $m = 0.05$ and $\theta' = 135^\circ$: piezoelectric coefficients d_{33}^* and d_h^* (in pCN^{-1}), piezoelectric coefficients g_{33}^* and g_h^* (in $10^{-2} \text{ V m N}^{-1}$) and squared figures of merit $(Q_{33}^*)^2$ and $(Q_h^*)^2$ (in 10^{-12} Pa^{-1}). Calculations have been made for the composites wherein the PMI matrix contains randomly distributed air pores, either spherical (b) or disc-like (c) ones, with volume fractions $0 < m_p \leq 0.3$ (see (a)).

Along with variations of the properties in the FC rods one can describe the effect of the Poisson ratio of the matrix $\nu^{(2)} = -s_{12}^{(2)}/s_{11}^{(2)}$ on the effective properties in the 1–3-type composite. Smith first showed [11] that considerable enhancement of the hydrostatic electromechanical coupling factor $k_h^* = d_h^*/(s_h^{*E} \varepsilon_{33}^{*\sigma})^{-1/2}$ (about 4–5 times where s_h^{*E} is the hydrostatic elastic compliance at $E = \text{const}$) and other effective parameters of the composite could be attained by decreasing the Poisson ratio $\nu^{(2)}$ of a hypothetical polymer matrix from 0.3 to –0.9.

In this paper we consider an auxetic polymer matrix for which the elastic properties have been determined in the experimental work [31]. These properties and the $\nu^{(2)}$ value could be varied, for example, by the presence of air pores in the PMI matrix. To satisfy conditions for subsequent averaging (a procedure suitable for ‘a composite in a composite’), we assume that the matrix contains air pores with sizes which are considerably larger than those of the microstructural elements in auxetic PMI, but considerably less than the radius of each FC rod embedded in this matrix. Such an interconnection between the sizes assumed could be attained

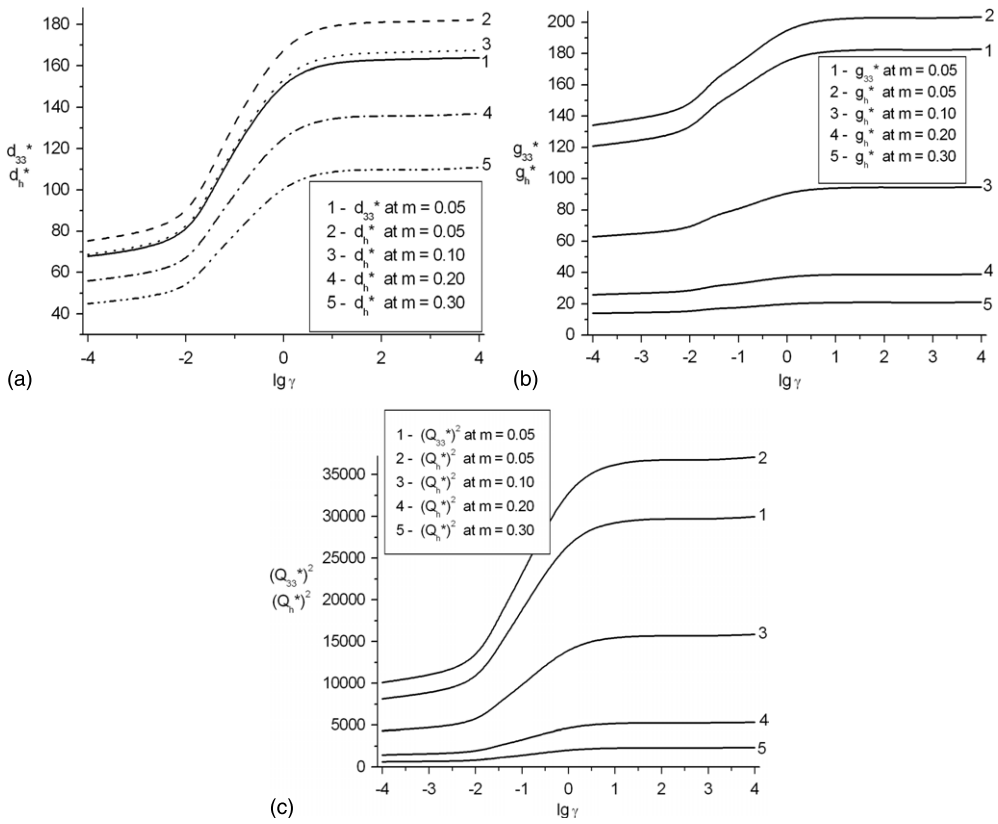


Figure 4. Effective parameters $\Phi^*(\lg \gamma)$ calculated for the 1–3-type BT FC/auxetic PMI composites at $m = \text{const}$: piezoelectric coefficients d_{33}^* and d_h^* ((a) in pCN⁻¹), piezoelectric coefficients g_{33}^* and g_h^* ((b) in mV m N⁻¹) and squared figures of merit $(Q_{33}^*)^2$ and $(Q_h^*)^2$ ((c) in 10⁻¹⁵ Pa⁻¹).

by the creation of a nano-sized auxetic structure and next a micro-sized porous structure. In this case the elastic and dielectric properties ($c_{ab}^{(2)}$ and $\varepsilon_{pp}^{(2)}$) in the polymer matrix with the randomly distributed air pores (e.g. spherical or disc-like) are determined [32] as a function of the porosity m_p . In our evaluation the disc-like pores are approximated by spheroids being described by an equation $(x_1/a_1)^2 + (x_2/a_1)^2 + (x_3/a_3)^2 = 1$ relative to the axes of a rectangular co-ordinate system. The semi-axes of the spheroid a_j obey the condition $a_3/a_1 = 10^{-2}$.

Examples of the $\nu^{(2)}(m_p)$ dependence are shown in figure 3(a). The corresponding porous and auxetic PMI matrix influences the effective parameters of the PZT-based composite as shown in figures 3(b) and (c). It is evident that the formation of the disc-like air pores in the PMI matrix results in a pronounced change in $\nu^{(2)}$ at $m_p < 0.1$ only (see curve 2 in figure 3(a) and, as a consequence, influences the effective parameters of the 1–3 composite (figure 3(c)) more actively in comparison with the case of the spherical pores in the matrix. A small increase in $\Phi^*(\nu^{(2)})$ (curves 3 and 5 in figures 3(b) and (c)) is caused by lowering $\varepsilon_{33}^{*\sigma}$ of the composite on averaging m_p and $\nu^{(2)}$. At the same time a small decrease in $\Phi^*(\nu^{(2)})$ (curves 2, 4 and 6 in figures 3(b) and (c)) is associated with the decrease in $(d_h^* - d_{33}^*)|_{m \ll 1}$ and $s_{12}^{(2)}$ (see equation (1)). Figure 3 contains data on the PZT-based composite only, but similar behaviour of the effective parameters $\Phi^*(\nu^{(2)})$ is also observed in the PCT-based composite at $m \ll 1$.

As follows from the data presented in figure 3, the porous structure in the isotropic PMI matrix influences the Poisson ratio $\nu^{(2)}$, but does not result in considerable improvement in the

piezoelectric characteristics of the studied composites. It is notable that anisotropic porous polymer matrices with various $s_{12}^{(2)}/s_{11}^{(2)}$ and $s_{13}^{(2)}/s_{33}^{(2)}$ ratios [7–9] enable achieving large values of hydrostatic parameters (d_h^* , g_h^* , $(Q_h^*)^2$ and k_h^*) of the 1–3-type composites.

The studied FC/auxetic PMI composites show some advantages over the 1–3 relaxor-ferroelectric single-crystal/araldite composites from the recent work [33]. According to the data [33], the largest values of the piezoelectric coefficients g_{33}^* and g_h^* are 519 mV m N^{-1} and 140 mV m N^{-1} , respectively. These values are attained in the $0.58 \text{ Pb}(\text{Mg}_{1/3}\text{Nb}_{2/3})\text{O}_3\text{--}0.42 \text{ PbTiO}_3$ single-crystal/araldite composite at the volume fraction of the single-crystal component $m_{sc} = 0.024$. Our results shown in figures 2(b) and (e) suggest that the relatively large g_{33}^* and g_h^* values can be attained in the presence of the auxetic matrix reinforced by the highly poled FC rods at volume fractions of $m \leq 0.1$. Furthermore, the $(Q_h^*)^2$ values calculated for the PZT-based composite (figure 2(f)) at $m < 0.1$ and $\Theta' > 120^\circ$ are larger than $(Q_h^*)^2$ measured on a related PZT/foamed polymer composite [6] with 1–3–0 connectivity. It should be mentioned that the 1–3 FC/polymer composites with low volume fractions m (approximately 0.033, 0.066, etc) have been manufactured [34], and features of such manufacturing might be taken into consideration when creating the 1–3-type FC / auxetic polymer composites.

3.2. Results for BT-based composites

A monotonic increase in the effective parameters of the composite is also observed as the mobility of the 90° domain walls in the BT grains increases (figure 4). The hydrostatic parameters d_h^* , g_h^* and $(Q_h^*)^2$ of the BT FC/auxetic PMI composite (figure 4) are varied in a wide range mainly due to the significant changes in d_{31}^* and g_{31}^* . It is worth noting that the zigzag-like curves shown in figure 3 resemble the $|s_{ab}^{(1),E}|$, $|d_{ij}^{(1)}|$ and $\varepsilon_{pp}^{(1),\sigma}$ curves calculated in the work of [28] for the BT FC in the range of $-4 \leq \lg \gamma \leq 4$. The large squared figures of merit $(Q_{33}^*)^2$ and $(Q_h^*)^2$ (figure 4(c)) are attained primarily due to considerable piezoelectric activity of the composite: values of its piezoelectric coefficients d_{33}^* and d_h^* are over 100 pC N^{-1} in the wide γ range (see figure 4(a)). Such properties offer some advantages over the performance of the PTC- or PZT-based composites. However, the piezoelectric coefficients g_{33}^* and g_h^* of the BT-based composite (figure 4(b)) are lower than the similar parameters of the PTC- and PZT-based composites (figures 2(b) and (e)). The low g_{33}^* and g_h^* values are primarily due to the high values of the dielectric constant $\varepsilon_{33}^{*\sigma}$ of the BT FC: according to the data [28] these values are about 10–20 times larger than those predicted for the PCT or PZT FCs on the basis of data from tables 1 or 2, respectively.

Finally, figure 5 shows examples of the volume fraction dependence of the studied parameters of the BT-based composite with a high 90° domain-wall mobility within ceramic grains. It is seen that at small volume fractions m (< 0.05) the elastic compliance $s_{12}^{(2)} > 0$ of the auxetic polymer promotes the condition $d_h^* > d_{33}^*$ (figure 5(a)) despite the negative contribution from the competing item being proportional to $d_{31}^{(1)}/d_{33}^{(1)}$ (see equation (1)). Maxima of g_{33}^* , g_h^* , $(Q_{33}^*)^2$ and $(Q_h^*)^2$ take place at $0 < m < 0.01$ (figures 5(b) and (c)); however, the values of these effective parameters remain relatively large in the range of $0.01 < m < 0.05$. It is believed that the volume fraction range of $0.03 < m < 0.05$ will be of interest for piezotechnical applications of the studied 1–3-type composite.

4. Conclusions

This study emphasises the important role of domain-orientation effects in improving the piezoelectric activity, sensitivity, figures of merit and other parameters of the 1–3-type FC/auxetic polymer composites. The effective piezoelectric properties and related parameters

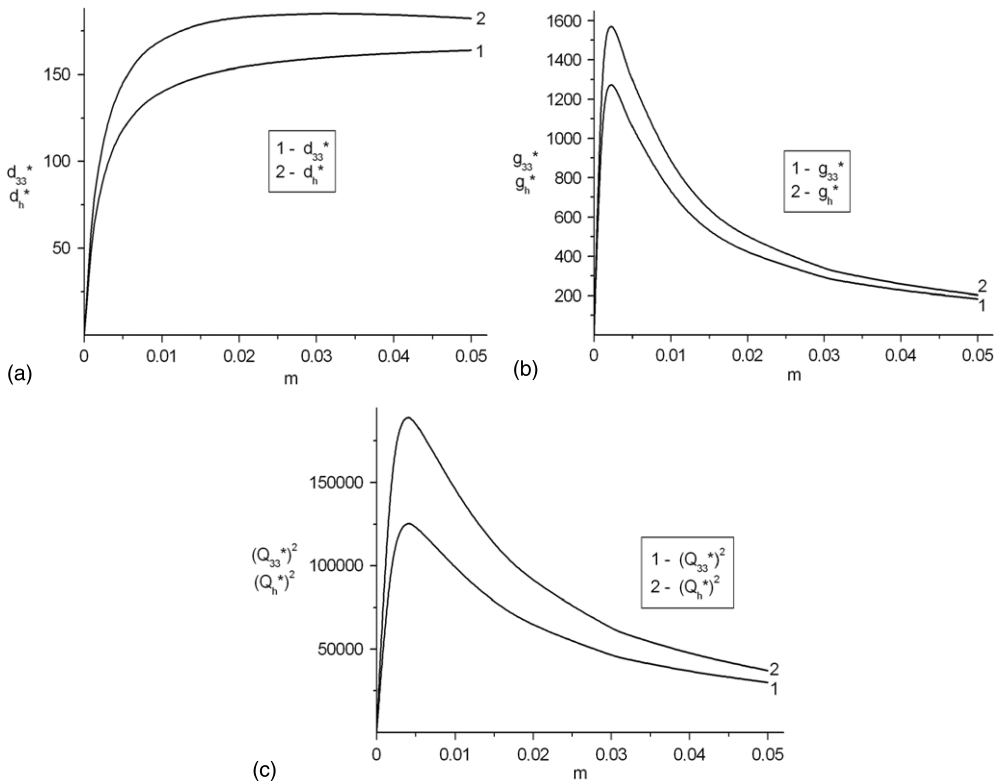


Figure 5. Effective parameters $\Phi^*(m)$ calculated for the 1–3-type BT FC/auxetic PMI composites at $\lg \gamma = 4$: piezoelectric coefficients d_{33}^* and d_h^* ((a) in pCN^{-1}), piezoelectric coefficients g_{33}^* and g_h^* ((b) in mVmN^{-1}) and squared figures of merit $(Q_{33}^*)^2$ and $(Q_h^*)^2$ ((c) in 10^{-15}Pa^{-1}).

of these composites can be improved due to the rotation of the spontaneous polarisation vector \mathbf{P}_s or the 90° domain-wall displacements in the ceramic grains. The auxetic polymer matrix with the negative Poisson ratio promotes the large values of the hydrostatic parameters of the composites studied in this work, and it is possible to attain $d_h^* > d_{33}^*$ and positive values of d_{31}^* . The competition between the items associated with the piezoelectric anisotropy of FC and elastic properties of polymer (i.e. $d_{31}^{(1)}/d_{33}^{(1)}$ and $s_{12}^{(2)}$ in equation (1)) influences the hydrostatic response and interconnections between d_{33}^* and d_h^* or g_{33}^* and g_h^* . As a consequence, different parameters (e.g. g_{33}^* , g_h^* and $(Q_h^*)^2$) at small volume fractions of FC become larger than the similar parameters of the 1–3-type composites studied earlier. This implies that low FC volume fractions and high polymer fractions should be considered to maximise the potential benefits of utilising auxetic polymers. These results can be of value for those manufacturing the advanced piezocomposites and predicting the effective parameters of these composites.

Acknowledgments

The authors would like to thank Professor R Stevens (University of Bath, UK) and Professor A E Panich (Southern Federal University, Russia) for their continued interest in the research problems. The work was partially supported by the EPSRC Platform Grant for the Centre for Power Transmission and Motion Control (GR/S64448/01), and this support is acknowledged by the authors.

References

- [1] Chan H L W and Unsworth J 1989 *IEEE Trans. Ultrason., Ferroelectr. Freq. Control* **36** 434–41
- [2] Taunaumang H, Guy I L and Chan H L W 1994 *J. Appl. Phys.* **76** 484–9
- [3] Ritter T *et al* 2000 *IEEE Trans. Ultrason., Ferroelectr. Freq. Control* **47** 792–800
- [4] Klicker K A, Biggers J V and Newnham R E 1981 *J. Am. Ceram. Soc.* **64** 5–9
- [5] Shaulov A A, Smith W A and Ting R Y 1989 *Ferroelectrics* **93** 177–82
Smith W A and Auld B A 1991 *IEEE Trans. Ultrason., Ferroelectr. Freq. Control* **38** 40–7
- [6] Akdogan E K, Allahverdi M and Safari A 2005 *IEEE Trans. Ultrason., Ferroelectr. Freq. Control* **52** 746–75
- [7] Sigmund O, Torquato S and Aksay I A 1998 *J. Mater. Res.* **13** 1038–48
- [8] Gibiansky L V and Torquato S 1997 *J. Mech. Phys. Solids* **45** 689–708
- [9] Nelli Silva E C, Ono Fonseca J S and Kikuchi N 1997 *Comput. Mech.* **19** 397–410
- [10] Topolov V Yu and Turik A V 2001 *Tech. Phys.* **46** 1093–100
- [11] Smith W A 1991 *Proc. IEEE Ultrasonics Symp. (Lake Buena Vista, FL, USA, 8–11 December, 1991)* vol 1 (New York: IEEE) pp 661–6
- [12] Wang Y C and Lakes R S 2001 *J. Appl. Phys.* **90** 6458–65
- [13] Lakes R 1987 *Science* **235** 1038–40
- [14] Bondarenko E I, Topolov V Yu and Turik A V 1991 *Ferroelectr. Lett. Sec.* **13** 13–19
- [15] Turik A V, Topolov V Yu and Aleshin V I 2000 *J. Phys. D: Appl. Phys.* **33** 738–43
- [16] Rödel J and Kreher W S 2003 *J. Eur. Ceram. Soc.* **23** 2297–306
- [17] Mori T and Tanaka K 1973 *Acta Metall.* **21** 571–4
- [18] Dunn M L 1993 *J. Appl. Phys.* **73** 5131–40
- [19] Levin V M, Rakovskaja M I and Kreher W S 1999 *Int. J. Solids Struct.* **36** 2683–95
- [20] Grekov A A, Kramarov S O and Kuprienko A A 1989 *Mech. Compos. Mater.* **25** 54–61
- [21] Huang J H and Kuo W-S 1996 *Acta Mater.* **44** 4889–98
- [22] Gorish A V, Dudkevich V P, Kupriyanov M F, Panich A E and Turik A V 1999 *Piezoelectric device-making Physics of Ferroelectric Ceramics* vol 1 (Moscow: Radiotekhnika) (in Russian)
- [23] Topolov V Yu, Turik A V and Chernobabov A I 1999 *Crystallogr. Rep.* **39** 805–9
- [24] Feronov A D, Kuleshov V V, Dudkevich V P and Fesenko E G 1980 *Zh. Tekh. Fiz.* **50** 621–3 (in Russian)
- [25] Turik A V and Topolov V Yu 1997 *J. Phys. D: Appl. Phys.* **30** 1541–9
- [26] Ikeda T 1990 *Fundamentals of Piezoelectricity* (Oxford: Oxford University Press)
- [27] Smith W A 1993 *IEEE Trans. Ultrason., Ferroelectr. Freq. Control* **40** 41–9
- [28] Aleshin V I 1990 *Zh. Tekh. Fiz.* **60** 179–83 (in Russian)
- [29] Turik A V 1970 *Sov. Phys.—Solid State* **12** 688–93
Akcakaya E, Farnell G W 1988 *J. Appl. Phys.* **64** 4469–73
- [30] Aleshin V I 1987 *Kristallografiya* **32** 422–6 (in Russian)
- [31] Martz E O *et al* 1996 *Cell. Polym.* **15** 229–49
- [32] Dunn M 1995 *J. Appl. Phys.* **78** 1533–41
- [33] Bezas S V, Topolov Yu and Bowen C R 2006 *J. Phys. D: Appl. Phys.* **39** 1919–25
- [34] Choy S U, Chan H L W, Ng M W and Liu P C K 2004 *Integr. Ferroelectr.* **63** 109–15